Phase separation and clustering of an ABC transporter in *Mycobacterium tuberculosis*

Florian Heinkel[a,b], Libin Abraham[c], Mary Ko[d], Joseph Chao[c,d], Horacio Bach[d], Lok Tin Hui[b], Haoran Li[a,b], Mang Zhu[a,b], Yeou Mei Ling[b], Jason C. Rogalski[a], Joshua Scurll[e], Jennifer M. Bui[a,b], Thibault Mayor[a,b], Michael R. Gold[c], Keng C. Chou[f], Yossef Av-Gay[c,d], Lawrence P. McIntosh[a,b,f,1], and Jörg Gsponer[a,b,1]

[a]Michael Smith Laboratories, University of British Columbia, Vancouver, BC, Canada V6T 1Z4; [b]Department of Biochemistry and Molecular Biology, University of British Columbia, Vancouver, BC, Canada V6T 1Z3; [c]Department of Microbiology and Immunology, University of British Columbia, Vancouver, BC, Canada V6T 1Z3; [d]Department of Medicine, University of British Columbia, Vancouver, BC, Canada V6H 3Z6; [e]Department of Mathematics and Institute of Applied Mathematics, University of British Columbia, Vancouver, BC, Canada V6T 1Z2; and [f]Department of Chemistry, University of British Columbia, Vancouver, BC, Canada V6T 1Z1

Edited by Peter E. Wright, The Scripps Research Institute, La Jolla, CA, and approved July 10, 2019 (received for review December 4, 2018)

Phase separation drives numerous cellular processes, ranging from the formation of membrane-less organelles to the cooperative assembly of signaling proteins. Features such as multivalency and intrinsic disorder that enable condensate formation are found not only in cytosolic and nuclear proteins, but also in membrane-associated proteins. The ABC transporter Rv1747, which is important for *Mycobacterium tuberculosis* (*Mtb*) growth in infected hosts, has a cytoplasmic regulatory module consisting of 2 phosphothreonine-binding Forkhead-associated domains joined by an intrinsically disordered linker with multiple phospho-acceptor threonines. Here we demonstrate that the regulatory modules of Rv1747 and its homolog in *Mycobacterium smegmatis* form liquid-like condensates as a function of concentration and phosphorylation. The serine/threonine kinases and sole phosphatase of *Mtb* tune phosphorylation-enhanced phase separation and differentially colocalize with the resulting condensates. The Rv1747 regulatory module also phase-separates on supported lipid bilayers and forms dynamic foci when expressed heterologously in live yeast and *M. smegmatis* cells. Consistent with these observations, single-molecule localization microscopy reveals that the endogenous *Mtb* transporter forms higher-order clusters within the *Mycobacterium* membrane. Collectively, these data suggest a key role for phase separation in the function of these mycobacterial ABC transporters and their regulation via intracellular signaling.

ABC transporter | FHA domain | phase separation | nanoclustering

Phase separation of proteins and nucleic acids into liquid-like condensates has emerged as a fundamental mechanism for eukaryotic cellular organization on a nanometer to micrometer scale (1–3). Most notably, this phenomenon underpins the spontaneous formation of membrane-less organelles, such as nucleoli, P-bodies, and stress granules. Phase separation results from weak, reversible multivalent interactions between proteins and/or nucleic acids (4–6). Proteins prone to phase separation are typically enriched in repeats of interaction domains and/or intrinsically disordered (ID) regions. Given that phase separation is enabled by quite generic and prevalent features of proteins, it is not surprising that many diverse eukaryotic proteins (1) and, more recently, prokaryotic proteins (7) have been found to form condensates in vitro and in vivo. Although much remains to be discovered about the cellular functions of phase separation in the different kingdoms of life, it is clear that condensation can be controlled through changes in protein/nucleic acid concentrations, posttranslational modifications, and variations in environmental conditions, including pH, temperature, and ionic strength.

In addition to membrane-less organelles, phase separation can create "2-dimensional nanoclusters" of signaling proteins at the cell membrane, as exemplified by the T-cell receptor (8) and the Nephrin adhesion receptor (9) pathways. Such cooperative assembly of localized, concentrated protein complexes may lead to switch-like behaviors and amplification of cellular responses by the recruitment or exclusion of additional signaling factors. Whether phase separation at the cell membrane is a common phenomenon exploited by many signaling proteins remains to be established. Of particular interest is the behavior of transmembrane proteins such as receptors and transporters, many of which are known to oligomerize and/or occur in nanoclusters (10–12).

We recently characterized the cytoplasmic regulatory module of the *Mycobacterium tuberculosis* (*Mtb*) ATP-binding cassette (ABC) transporter that is encoded by the ORF *Rv1747* (13). This module consists of 2 phosphothreonine (pThr)-binding Forkhead-associated (FHA) domains connected by an ∼125-aa linker (Fig. 1*A*). The ID linker has low sequence complexity and contains several threonine residues that can be phosphorylated by multiple *Mtb* serine/threonine protein kinases (STPKs), including PknF. Rv1747$^{1–310}$, a construct spanning the regulatory module, is capable of intramolecular and intermolecular FHA/pThr interactions that lead to the formation of a variety of higher-order oligomers, depending on the linker phosphorylation state (13). Although implicated in the export of cell wall biosynthesis intermediates, the physiological cargo of Rv1747 is unknown (14). Nevertheless, Rv1747 contributes to *Mtb* virulence in a manner

Significance

Nanoclustering has emerged as an organization principle of membrane proteins. This form of compartmentalization has been observed in eukaryotes and, to a lesser extent, in bacteria. Bacterial membrane proteins in secretion systems often play central roles during host invasion. Here we reveal that an ABC transporter from *Mycobacterium tuberculosis* (*Mtb*), which is important for its growth in mice, compartmentalizes in the bacterial membrane. We demonstrate that the cytoplasmic region of this transporter has an intrinsic ability to phase-separate into mesoscale assemblies, and that this process is controllable via the action of the signal-integrating serine/threonine protein kinases and phosphatase in *Mtb*. Our findings suggest that phase separation can play a key role in the regulation of clustering and activity of membrane-bound bacterial proteins.

Author contributions: F.H., L.P.M., and J.G. designed research; F.H., L.A., M.K., J.C., H.B., L.T.H., H.L., M.Z., Y.M.L., and J.C.R. performed research; L.A., J.C., H.B., J.S., and J.M.B. contributed new reagents/analytic tools; F.H., L.A., T.M., M.R.G., K.C.C., Y.A.-G., L.P.M., and J.G. analyzed data; and F.H., L.A., Y.A.-G., L.P.M., and J.G. wrote the paper.

The authors declare no conflict of interest.

This article is a PNAS Direct Submission.

[1]To whom correspondence may be addressed. Email: mcintosh@chem.ubc.ca or gsponer@msl.ubc.ca.

This article contains supporting information online at www.pnas.org/lookup/suppl/doi:10.1073/pnas.1820683116/-/DCSupplemental.

Published online July 31, 2019.

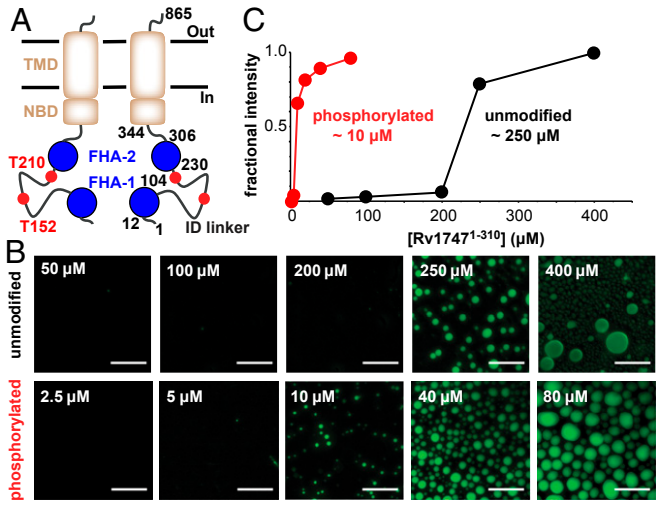

Fig. 1. Rv1747$^{1–310}$ undergoes phosphorylation-enhanced phase separation into liquid-like droplets in vitro. (*A*) Schematic representation of Rv1747 as a homodimer with the regulatory module (FHA domains, blue; reported PknF phospho-acceptor sites T152/T210 in the ID linker, red) appended to the core ABC transporter (transmembrane domain [TMD] and nucleotide binding domain [NBD], brown, with boundaries indicated). (*B*) Unmodified and phosphorylated Rv1747$^{1–310}$ phase-separated at different threshold concentrations. Shown are fluorescent images of unmodified (*Top*) and phosphorylated (*Bottom*) OG-Rv1747$^{1–310}$, taken at 120 min after removal from the concentration device or after the addition of 0.5 μM PknF and 100 μM ATP, respectively. (Scale bars: 40 μm.) (*C*) The indicated saturation concentrations for phase separation were quantified by fractional fluorescence intensity.

that requires the reported phospho-acceptors T152/T210 and the binding properties of the FHA domains (15), and thus most likely on its ability to oligomerize. We hypothesized that phase separation results from oligomerization of the regulatory module and mediates phosphorylation-dependent clustering of Rv1747 in the *Mtb* membrane.

In support of this hypothesis, we demonstrate here that the Rv1747 regulatory module undergoes reversible phase separation that is enhanced on phosphorylation by multiple *Mtb* STPKs. Phase separation is also exhibited by MSMEG_1642, the *Mycobacterium smegmatis* ortholog of Rv1747. Furthermore, we demonstrate phase separation of the regulatory module on supported lipid bilayers, as well as formation of dynamic foci when heterologously expressed in *M. smegmatis* and *Saccharomyces cerevisiae*. These observations all point to an evolutionarily conserved role of this phenomenon in the in vivo organization and regulation of mycobacterial ABC transporters. Consistent with this role, full-length Rv1747 forms foci in *M. smegmatis*, and superresolution single-molecule localization microscopy reveals that the transporter assembles into higher-order nanoclusters within the *Mtb* membrane.

Results

Rv1747$^{1–310}$ Cooperatively Phase-Separates on Phosphorylation. We previously demonstrated that the isolated FHA-1 and FHA-2 domains each bind with micromolar affinity to phosphopeptides corresponding to the mapped PknF phospho-acceptor sites T152 and T210 within the ID linker (13). In addition, NMR-monitored titrations revealed unambiguously the formation of intramolecular and intermolecular complexes when either the FHA-1 or FHA-2 domain was joined to the phosphorylated linker as a continuous polypeptide chain. Such weak, reversible multivalent interactions are a hallmark of phase-separating proteins. Consistent with phase separation, solutions of the construct Rv1747$^{1–310}$, spanning the full regulatory module, became visibly turbid on phosphorylation (13).

Using microscopy, we found that monodisperse samples of Rv1747$^{1–310}$ (50 μM) spontaneously formed spheroidal condensates with well-defined boundaries when phosphorylated by PknF (Fig. 1*B* and *SI Appendix*, Fig. S1). The condensates had diagnostic liquid-like properties, including growth in size over time, coalescence into large droplets (*SI Appendix*, Fig. S2), and diffusive exchange both within droplets (Fig. 2*A*) and from protein-depleted to protein-rich phases (*SI Appendix*, Fig. S3). Droplet formation by the PknF-treated protein was also cooperative, with a saturation concentration of ∼10 μM under the standardized conditions chosen for these studies (Fig. 1*C*). Although the necessity of phosphorylation was confirmed through control experiments without kinase, ATP, or Mg^{2+}, electrospray ionization mass spectrometry revealed that substoichiometric phosphorylation was sufficient to induce condensation of Rv1747$^{1–310}$ under these conditions (*SI Appendix*, Fig. S4). Phase separation was also impaired, but not fully abrogated, by alanine substitutions of the mapped (15) phospho-acceptors T152/T210. Residual levels of condensation likely resulted from phosphorylation of alternative linker residues (*SI Appendix*, Fig. S5). Indeed, mass spectrometry phospho-acceptor mapping revealed that besides T152, T116, T117, S161, and T169 were also phosphorylated by PknF (*SI Appendix*, Fig. S6), whereas the previously identified acceptor T210 was not confirmed.

Unmodified Rv1747$^{1–310}$ Also Undergoes Phase Separation. Further investigation revealed that nonphosphorylated Rv1747$^{1–310}$ also phase-separated, albeit at a significantly higher saturation concentration (∼250 μM) than the PknF-treated protein (Fig. 1 *B* and *C*).

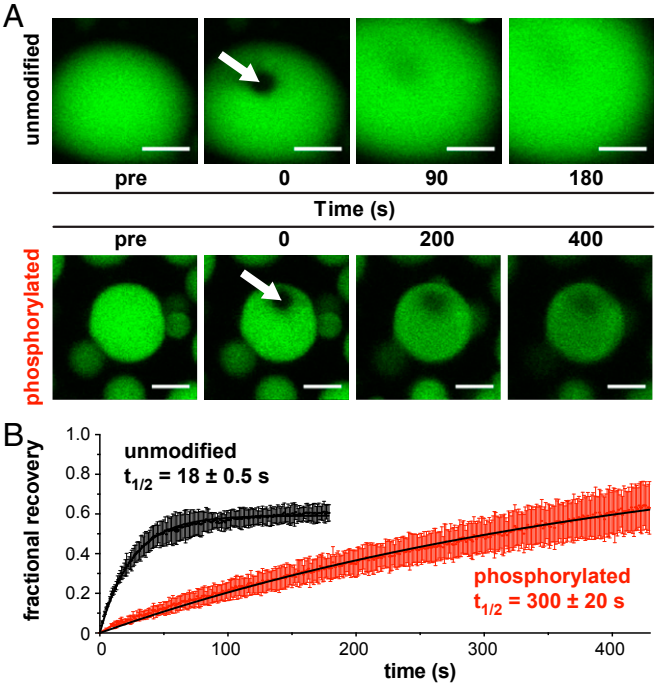

Fig. 2. Diffusive exchange of phase-separated Rv1747$^{1–310}$ slows on phosphorylation. (*A*) FRAP measurements of exchange at room temperature in droplets formed by unmodified OG-Rv1747$^{1–310}$ (>250 μM; *Top*) or phosphorylated OG-Rv1747$^{1–310}$ (50 μM treated with 0.5 μM PknF and 100 μM ATP; *Bottom*). The bleached sector at $t = 0$ is indicated by an arrow, followed by images obtained at 2 subsequent time points. (Scale bars: 5 μm.) Although fluorescence recovery is likely dominated by diffusive exchange within the droplet, exchange with surrounding liquid phase is also possible. (*B*) FRAP recovery was quantified by fitting the average normalized intensity (solid dots with SD bars) to a single exponential function (black lines) for 3 different droplets in 1 sample of either unmodified or phosphorylated Rv1747$^{1–310}$.

Neither the isolated FHA domains (13) nor the ID linker formed condensates at concentrations as high as 350 μM. Consistent with the latter, an algorithm based on potential pi–pi interactions predicted weak phase-separating behavior (*z*-score of 1.8) for the ID linker on its own (16). This suggests that nonspecific electrostatic interactions between the linker (theoretical pI 11.9) and the FHA domains (pI 6.4 and 5.0, respectively) may play an important role in phase separation. Consistent with this hypothesis, the saturation concentration of nonphosphorylated Rv1747$^{1–310}$ increased with ionic strength (*SI Appendix*, Fig. S7). Substoichiometric phosphorylation tips the balance to promote cooperative phase separation of Rv1747$^{1–310}$ at lower concentrations due to specific FHA domain/pThr binding.

We used fluorescence recovery after photobleaching (FRAP) to characterize the diffusive properties of phase-separated Rv1747$^{1–310}$. The initial recovery rate was more rapid in droplets formed by unmodified Rv1747$^{1–310}$ ($t_{1/2}$ = 18 ± 0.5 s) than those formed by phosphorylated Rv1747$^{1–310}$ ($t_{1/2}$ = 300 ± 20 s) (Fig. 2*B*). Although these data should be interpreted as semiquantitative, they clearly demonstrate that recovery of the mobile component is slowed by more than an order of magnitude on phosphorylation. Full fluorescence recovery was not observed, suggesting that a fraction of the condensed material is less mobile, as also has been observed for stress granules (17) and nucleoli (18) in vivo. Collectively, these measurements indicate that heterogenous types and numbers of multivalent interactions mediate phase separation by unmodified and phosphorylated Rv1747$^{1–310}$ and modulate the viscoelastic properties of the resulting condensates.

Phase Separation of Rv1747 Regulatory Module Is Evolutionarily Conserved. If phase separation plays a functional role, then it would be expected to be observed in homologous species. MSMEG_1642, the *M. smegmatis* ABC transporter ortholog of Rv1747, also has a putative regulatory module with 2 conserved FHA domains joined by a longer, more divergent ID linker (*SI Appendix*, Fig. S8). Consistent with evolutionary conservation, a construct spanning this module, MSMEG_1642$^{1–340}$, phase-separated in vitro. Phosphorylation by PknF also reduced the threshold concentration for MSMEG_1642$^{1–340}$ to form condensates (*SI Appendix*, Fig. S9).

Phase Separation of Rv1747 Is Reversibly Modulated by the Serine/Threonine Phosphatase and Additional Kinases of *Mtb*. Functionally relevant phase separation of Rv1747 should be reversible via dephosphorylation and induced by other STPKs that exhibit extensive cross-talk for mycobacterial signaling (19). Indeed, PstP, the sole serine/threonine phosphatase present in *Mtb*, dissolved PknF-induced Rv1747$^{1–310}$ droplets (Fig. 3*A*). *PknF* resides in the same operon as Rv1747, and this "cognate" kinase induced phase separation, as shown above. *Mtb* also expresses several related STPKs. We found that the purified catalytic domains of 9 of these also phosphorylated Rv1747$^{1–310}$ in vitro, although with varying levels of efficiency and specificity for the mapped PknF phospho-acceptors T152/T210 and additional unmapped sites. Importantly, most of these STPKs were able to induce phase separation of Rv1747$^{1–310}$ (Fig. 3*B* and *SI Appendix*, Fig. S10). This is consistent with both the promiscuity and overlapping specificity of the STPKs for their substrates (20), and also with the observation that even substoichiometric phosphorylation of Rv1747$^{1–310}$, as well as the T152A/T210A mutant, by PknF enhanced droplet formation.

Phase Separation Regulating Enzymes Colocalize to Rv1747$^{1–310}$ Droplets. Recent studies have revealed that liquid-like protein condensates can act as biomolecular filters (21). In the case of condensates formed by members of the T-cell signaling cascade, kinases that enhance signaling are enriched in condensates,

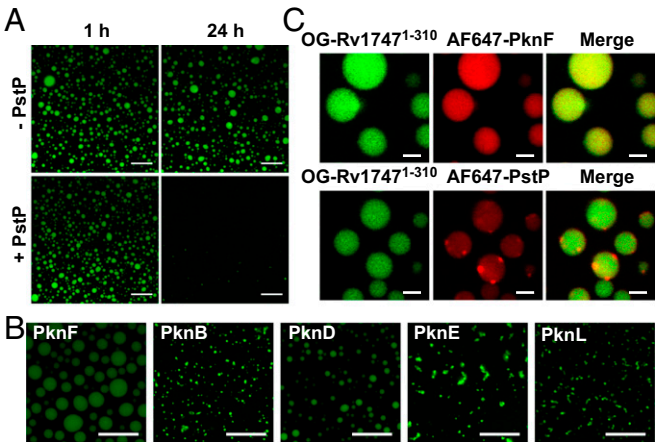

Fig. 3. Rv1747 phase separation is regulated by the *Mtb* STPKs and phosphatase. (*A*) PstP dissolved PknF-induced Rv1747$^{1–310}$ droplets. Condensates of 50 μM OG-Rv1747$^{1–310}$ were formed at room temperature in buffer containing 100 μM ATP and 0.5 μM PknF. After 120 min, the PstP phosphatase domain (5 μM) was added to 1 of 2 samples, and fluorescent images were recorded at the indicated time points. (Scale bars: 20 μm.) Dissolution occurred slowly, likely due to the competing activity of PknF with ATP still present in the sample and the requirement for only substoichiometric phosphorylation to induce cooperative phase separation. (*B*) Fluorescence images of OG-Rv1747$^{1–310}$ droplets induced by 5 *Mtb* STPKs (0.5–2 μM kinase domain plus 100 μM ATP) (Scale bars: 20 μm.) With a starting concentration of 10 μM, any unmodified Rv1747$^{1–310}$ was below its threshold concentration for phase separation. (See also *SI Appendix*, Fig. S10.) (*C*) The PknF and PstP catalytic domains colocalized to OG-Rv1747$^{1–310}$ droplets. After formation with nonlabeled PknF (0.5 μM with 100 μM ATP), 0.05 μM AF647-PknF (*Top*) or AF647-PstP (*Bottom*) was added. Images of OG (green) and AF647 (red) fluorescence were overlaid to monitor colocalization. (Scale bars: 2 μm.)

whereas phosphatases that oppose condensation are excluded (8). We tested whether the enzymes regulating phase separation of Rv1747$^{1–310}$ also show preferential interactions with respect to the resulting condensates. Both AF647-labeled PknF and PstP were enriched in phosphorylated OG-Rv1747$^{1–310}$ droplets (Fig. 3*C*). However, unlike uniformly-distributed PknF, fluorescently labeled PstP appeared as foci on the surface of the droplets. This points to the presence of coexisting phases that are differentially penetrated and enriched in components of this *Mtb* signaling system (17). This might originate from different interaction mechanisms with the highly concentrated Rv1747$^{1–310}$. These mechanisms could include the association of the enzyme active sites with the linker phospho-acceptor residues, as well as the binding of pThr residues in autophosphorylated PknF to the FHA domains (22, 23). It is important to note that Rv1747$^{1–310}$ droplets do not have an inherent property to recruit any protein. Whereas a single chain variable fragment (scFv) selected via phage display screening for binding to the FHA-1 domain of Rv1747 does colocalize to droplets, this is not the case for a nonspecific scFv (see below).

Rv1747$^{1–310}$ Phase-Separates When Tethered to Lipid Bilayers. Rv1747$^{1–310}$ corresponds to the cytosolic regulatory module of a membrane-spanning ABC transporter. Thus, we tested whether phase separation still occurs in a membrane-associated context by anchoring His_6-tagged OG-Rv1747$^{1–310}$ to a supported lipid bilayer on a glass coverslip. The pseudo-2D concentration of protein on the surface of this model membrane is set by the fraction of nitrilotriacetic acid-modified lipid [DGS-NTA(Ni^{2+})] present. In this system, unmodified Rv1747$^{1–310}$ readily separated into condensates above a sharp cooperative concentration threshold (Fig. 4*A*). The membrane-bound condensates also showed diffusive

exchange, with FRAP recovery times comparable to those exhibited by droplets of the nonphosphorylated protein in solution (*SI Appendix*, Fig. S11). This implies that phase separation of the regulatory module could drive the clustering of wild-type Rv1747 in its native context.

Rv1747$^{1–310}$ Forms Dynamic Foci When Expressed in *S. cerevisiae* and *M. smegmatis*. To assess the behavior of the regulatory module under native-like conditions, we expressed Rv1747$^{1–310}$, tagged with the fluorescent protein msfGFP, in *S. cerevisiae*. In contrast to the uniform distribution of a msfGFP-only control, yeast cells expressing msfGFP-Rv1747$^{1–310}$ had dense foci (Fig. 4*B* and *SI Appendix*, Fig. S12). These foci displayed properties consistent with phase separation, such as coalescence (Movie S1) and recovery of fluorescence after bleaching (*SI Appendix*, Fig. S12).

We also carried out live cell imaging of *M. smegmatis* expressing the regulatory module tagged with the fluorescent protein mEos2. Whereas mEos2 signals were mainly uniformly distributed, mEos2-Rv1747$^{1–310}$ formed multiple discrete foci along the length of the bacterium (Fig. 4*C* and *SI Appendix*, Fig. S13*A*).

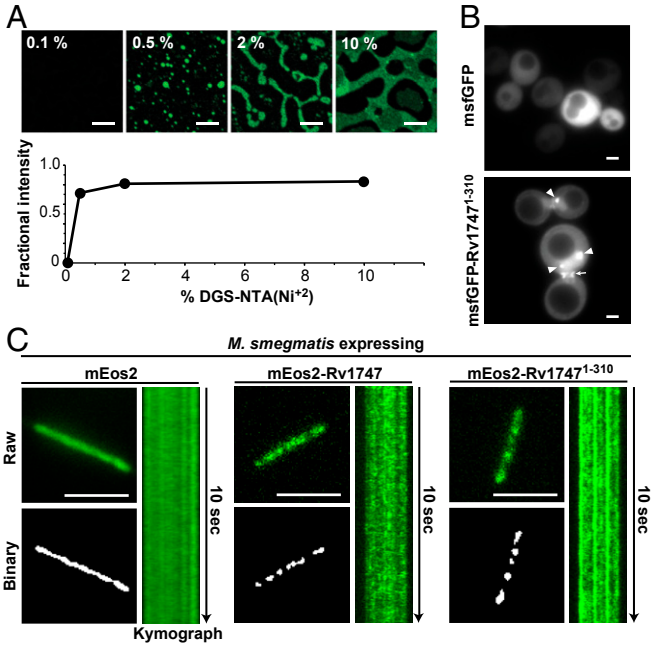

Fig. 4. Rv1747$^{1–310}$ undergoes spontaneous clustering on supported lipid bilayers and in vivo. (*A*) Fluorescence images of nonphosphorylated His_6-tagged OG-Rv1747$^{1–310}$ anchored to supported lipid bilayers containing DGS-NTA(Ni^{2+}). (Scale bars: 8 μm.) Phase separation was quantified by the fractional fluorescence intensity vs. weight percentage of the NTA(Ni^{2+}) lipid, which sets the pseudo-2D concentration of anchored Rv1747$^{1–310}$. At higher DGS-NTA(Ni^{2+}) levels, a characteristic spinodal decomposition (9) of the membrane-anchored droplets was seen. (*B*) Fluorescent images of yeast cells expressing msfGFP or msfGFP-Rv1747$^{1–310}$. Arrowheads indicate dense foci of msfGFP-Rv1747$^{1–310}$, and the arrow designates increased fluorescence intensities at the bud neck. Foci formation coincided with greater expression levels of msfGFP-Rv1747$^{1–310}$, likely driven by a higher plasmid copy number in these cells. Bud neck localization may be due to binding of the Rv1747$^{1–310}$ FHA domains to similar targets recognized by the endogenous FHA-containing protein Rad53 (33). (*C*) Representative total internal reflection fluorescence (TIRF) micrographs of live *M. smegmatis* expressing the indicated proteins. (Scale bars: 5 μm.) (*Top Left*) Raw images from the first frame of Movie S2 were analyzed using Icy Bioimaging particle detection software (*Methods*). (*Bottom Left*) Foci above the detection criteria are shown in the binary image output of the software. (*Right*) Kymographs illustrating the time evolution of fluorescence signals across the length of the bacterium in the raw image.

We analyzed the signals using a 2D space-time plot (kymograph), which confirmed that the foci were stable and present throughout the duration of imaging (Fig. 4*C* and Movie S2). The expressed mEos2-Rv1747$^{1–310}$ also underwent diffusive exchange as detected by FRAP (*SI Appendix*, Fig. S13 *B* and *C*). Together, these findings demonstrate the Rv1747 regulatory module phase-separates both on model membranes and in live cells.

Rv1747 Forms Clusters in Mycobacterial Membranes. To investigate whether our discovery of regulatory module phase separation translates to clustering of full-length Rv1747 in vivo, we undertook two types of experiments. First, we expressed mEso2-tagged Rv1747 in *M. smegmatis.* Similar to the regulatory module, the full-length protein formed foci (Fig. 4*C* and *SI Appendix*, Fig. S13*A*); however, these foci were more dynamic, as they assembled and disassembled during the time scale of imaging (Fig. 4*C* and Movie S2). Interestingly, a similar difference between a full-length protein and a phase-separation–inducing module was recently observed for RNase E in *Caulobacter crescentus* and linked to its catalytic activity (7). Thus, the presence of the transmembrane and nucleotide binding domains may modulate the dynamics of the foci formed by full-length Rv1747.

In a second set of experiments, we used superresolution microscopy to investigate whether Rv1747 forms higher-order assemblies in its native environment in *Mtb*. To do so, we labeled fixed, permeabilized *Mtb* with an AF647-conjugated single chain variable fragment (scFv) that had been selected via phage display screening for binding to the FHA-1 domain of Rv1747 (Fig. 5*A* and *SI Appendix*, Fig. S14*A*). Single-molecule localization microscopy (SMLM) images of the stained *Mtb* cells showed that the fluorescent anti-Rv1747 scFv was distributed nonuniformly in nanoclusters (Fig. 5*B* and Movie S3). More than one-half of these localizations were organized into clusters with substantially larger than expected areas from a highly generous estimation of the dimensions of a single Rv1747 transporter molecule (Fig. 5 *C* and *D* and *SI Appendix*, Fig. S15). This is consistent with higher-order assembly of this transporter within the bacterial membrane in vivo. As key controls, staining of *Mtb* was not observed with a nonspecific scFv, and staining of a Δ*rv1747* deletion strain was not observed with the anti-Rv1747 scFv (*SI Appendix*, Fig. S14 *B* and *C*).

Discussion

The ABC transporter Rv1747 is a virulence factor that has been implicated in transporting intermediates of the cell wall biosynthesis pathway across the *Mtb* membrane (14). Deletion of Rv1747 leads to *Mtb* growth defects in macrophages and infected mice. Importantly, the activity of Rv1747 and its contributions to virulence are dependent on interactions mediated by its regulatory module FHA domains and the linker phospho-acceptor threonines (15). In this study, we show that this module has an intrinsic ability to form condensates at high concentrations, possibly mediated by weak electrostatic interactions of the structured FHA domains with the unmodified ID linker. Phosphorylation of 1 or more linker threonines dramatically reduces the saturation concentration for phase separation of Rv1747$^{1–310}$, likely through the synergy of these intrinsic properties with specific intramolecular and intermolecular FHA domain/pThr interactions (13).

We postulate that phase separation plays an important role in the function and regulation of Rv1747. This is supported by our finding that condensation of the regulatory module of the orthologous ABC transporter in *M. smegmatis*, MSMEG_1642, is conserved. Moreover, phosphorylation-enhanced phase separation of Rv1747$^{1–310}$ is reversible via addition of the *Mtb* phosphatase PstP and inducible to varying degrees via many of the *Mtb* regulatory STPKs. Therefore, it ties seamlessly into the intricate phospho-signaling network of the bacterium. However,

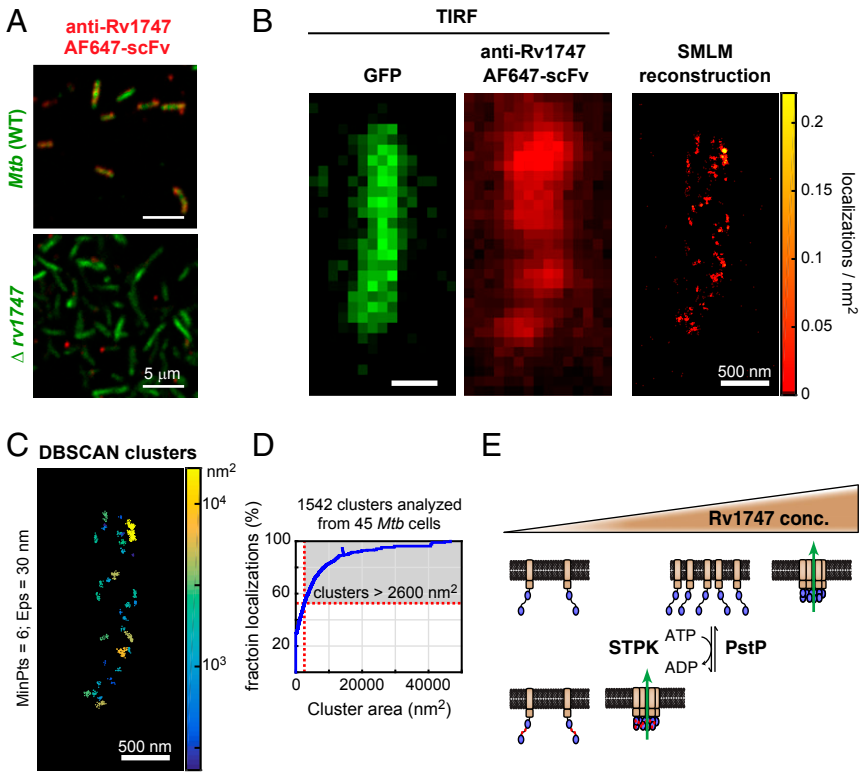

Fig. 5. Nanoclusters of Rv1747 in *Mtb*. (*A*) Rv1747-specific AF647-scFv stained cell wall-labeled (green) *Mtb*, but not Δ*rv1747* Erdman (*SI Appendix*, Fig. S14). (*B*) Representative TIRF micrographs of GFP (*Left*) and anti-Rv1747 AF647 (*Middle*) from a single *Mtb* cell acquired before superresolution imaging. (*Right*) SMLM reconstructions of anti-Rv1747 AF647-scFv localizations, depicted as a color-coded density plot. (Scale bar: 500 nm.) (*C*) Single-molecule localizations were clustered in 3D using DBSCAN (32). The depicted clusters are color-coded by area. Each cluster contains at least 6 localizations (MinPts) within 30 nm (Eps) of each other. (*D*) Distribution function showing the cumulative fraction of all localizations from 45 *Mtb* cells. The *y*-intercept is the fraction of nonclustered localizations. Close to one-half (47%) of the localizations were organized into clusters larger than 2,600 nm^2, the estimated maximal area occupied by an Rv1747 molecule. (*E*) Model for phosphorylation-enhanced clustering and regulation of Rv1747. The transporter (core ABC structure, brown) clusters due to the concentration-dependent phase separation of the regulatory module (FHA domains, blue). This may increase the transporter activity (green arrow) of Rv1747 via an undefined mechanism. Phosphorylation (red circles) by *Mtb* STPKs reduces the saturation concentration for clustering (upper triangle). Additional interactions with regulatory proteins or transporter substrates could modulate the saturation concentration.

phosphorylation of the Rv1747 linker at T152 and other sites by various STPKs under nonphysiological in vitro conditions might not accurately reflect the in vivo activities of these kinases.

Further support for a functional role of condensation lies in our observation that PknF and PstP colocalize differently with phase-separated Rv1747$^{1–310}$. In contrast to the homogenous distribution of PknF, PstP forms foci at the interface between the main Rv1747$^{1–310}$-rich phase and the protein-depleted surrounding buffer. Multiphase immiscibility, which increasingly appears to be a common feature of cellular condensates (3, 18), potentially limits the ability of PstP to dissolve condensates of phosphorylated Rv1747$^{1–310}$. In the cellular context, the reduced accessibility of the condensate-dissolving phosphatase may increase and prolong the regulatory impact of phosphorylation-enhanced Rv1747 phase separation (8).

Based on these in vitro findings, we propose a working model that connects phase separation and transporter activity via its clustering in the membrane (Fig. 5*E*). Rv1747 has an intrinsic ability to cluster at high concentrations on the surface of the *Mtb* membrane. Signaling-mediated phosphorylation of the linker by STPKs serves as a "multivalency dial" by enabling specific FHA domain/pThr interactions to promote Rv1747 clustering. Dephosphorylation by PstP reverses this effect. Phase separation-mediated clustering could potentially increase transport efficiency due to allosteric activity regulation, amplification of signals by selectively filtering substrates, and/or formation of a scaffold for interactions with additional components of the cell wall biosynthesis pathways (14). In this model, STPKs/PstP allow rapid and reversible activation/deactivation of Rv1747 on initial exposure to challenging environments in infected macrophages. Increased expression of Rv1747, or perhaps increased local concentration driven by additional regulatory factors, may also lead to phosphorylation-independent phase separation. This would enable a sustained and prolonged response that is independent of STPK-mediated signaling.

In accordance with our model, we found that the regulatory module also phase-separated in the context of supported lipid bilayers and formed foci that displayed properties consistent with phase separation when expressed heterologously in *S. cerevisiae* and *M. smegmatis*. Most importantly, full-length Rv1747 also formed foci in *M. smegmatis*, and native Rv1747 was nonuniformly localized into nanoclusters at the *Mtb* membrane. The clusters exhibited a distribution of sizes well exceeding the estimated dimensions of a single Rv1747 transporter. Previous reports have shown that some ABC membrane proteins can oligomerize (24, 25) and form nanoclusters (26), potentially to change substrate specificities or to allosterically regulate activity. Our findings provide evidence of nanoclustering by a bacterial ABC transporter.

Nanoclustering has emerged as a general organizing principle of membrane proteins, particularly receptors. Indeed, advances in microscopy and fluorescence spectroscopy have enabled the detailed characterization of the clustering of numerous eukaryotic and bacterial membrane proteins (11, 27, 28). Recently, phase separation of adaptor molecules binding to the cytoplasmic tails of the membrane proteins has been identified as a mechanism that could lead to nanoclustering (8). Our results are certainly not conclusive that phase separation of the regulatory module drives the clustering of full-length Rv1747. Membrane lipid organization, the tendency of the transmembrane segment to oligomerize, and/or interactions with other partner molecules could also contribute to clustering (11, 12, 29). Nonetheless, our data unambiguously demonstrate that the Rv1747 regulatory module can phase-separate in vitro and in vivo. Thus, it is likely that phase separation contributes to the identified self-organization of Rv1747 even when acting in conjunction with other cluster-promoting factors (12).

In summary, we reveal that the regulatory module of the *Mtb* ABC transporter Rv1747 undergoes phosphorylation-enhanced phase separation triggered by multiple STPKs. Reversibility via phosphatase treatment, along with the conserved behavior of an

orthologous protein from *M. smegmatis*, suggest that this phase separation is an evolutionarily-preserved mechanism to assemble multiple Rv1747 transporter molecules into the nanoclusters that we observed via superresolution microscopy. Whether phase separation plays a dominant and widespread role in the assembly of bacterial membrane proteins remains to be determined. Regardless, it is likely that phase separation, initially discovered in eukaryotes, is involved in the organization and function of macromolecular bacterial systems.

Methods

More detailed descriptions of the materials and methods used in this study are provided in *SI Appendix*. A brief summary is provided here.

Protein Expression and Purification. The regulatory modules of Rv1747 and MSMEG_1642, the catalytic domains of the *Mtb* phosphatase PstP and STPK kinases, and the scFv protein constructs were expressed in *Escherichia coli* and purified by standard chromatography methods. For fluorescence detection, $Rv1747^{1–310}$ was labeled with Oregon Green (OG), and $PstP^{1–240}$, $PknF^{1–292}$, and the scFvs were labeled with Alexa Fluor 647 (AF647).

Phase Separation of $Rv1747^{1–310}$. Phase separation of the investigated system depends on numerous factors, such as protein concentration, incubation time with a kinase, and sample conditions, including temperature. For consistency, we developed standard protocols for experiments performed in this study. Typically, samples of OG-$Rv1747^{1–310}$ at the indicated concentrations were incubated at 22 °C for 120 min with specified molar ratios of the STPK kinase domains in 20 mM sodium phosphate, 100 mM NaCl, and 5 mM $MgCl_2$ at pH 7.4. For example, to ensure low-level phosphorylation of 50 μM OG-$Rv1747^{1–310}$, the PknF:OG-$Rv1747^{1–310}$ molar ratio was 1:100 with 100 μM ATP. In the case of unmodified OG-$Rv1747^{1–310}$, samples were slowly concentrated at 22 °C and 2,000 × *g* in 10-kDa molecular weight cutoff centrifugal filters (EMD Millipore). At frequent intervals, centrifugation was stopped, the sample was thoroughly resuspended, and the concentration was determined using UV-absorbance.

Imaging of $Rv1747^{1–310}$ and $MSMEG\_1642^{1–340}$ Droplets. Differential interference contrast (DIC) and fluorescence microscopy were performed using an Olympus FV1000 inverted confocal microscope with a UplanSApo 60×/1.35 numerical aperture oil immersion objective. All images were acquired at ∼22 °C while maintaining consistent lamp/laser power, exposure time, gain, and offset. Images were processed and analyzed with ImageJ. To quantify phase separation, the integrated intensity of pixels classified as droplets was divided by the integrated intensity of all pixels within an image.

SMLM of Labeled *Mtb*. GFP-expressing *Mtb* cells were settled on poly-L-lysine–coated coverslips for 1 h at 4 °C and then fixed with PBS containing 4% paraformaldehyde for 30 min. The *Mtb* samples were then treated with lysozyme (2 mg/mL in H_2O) for 30 min at 37 °C, followed by Triton X-100 (0.1% in H_2O) for 5 min at ∼22 °C. After washing in PBS, the sample was blocked with 10% normal goat serum in PBS for 30 min and then stained with the AF647-conjugated Rv1747-specific scFv for 1 h at 22 °C. The latter was obtained by biopanning an optimized M13 bacteriophage phagemid library presenting $\sim 10^9$ different scFv clones against $Rv1747^{1–156}$ (FHA-1 and partial linker). SMLM imaging was carried out using a custom-built microscope with a real-time sample drift-stabilization system as described previously (30, 31). Custom software written in MATLAB (MathWorks) was used to reconstruct the SMLM images (30). Clustering of SMLM localizations was performed in 3-dimensions using DBSCAN (32).

ACKNOWLEDGMENTS. We thank Guy Tanentzapf and Darius Camp for FRAP instrumentation access, Gagandeep Narula for microbiology help, Erich Kuechler for predictions, Sahile Henok Asfaw for synthesis of the trehalose probe for tagging mycobacteria, and Dr. John Chan (Albert Einstein College of Medicine) for the *Mtb* Δ*rv1747* mutant. This study was funded by the Canadian Institutes for Health Research (MOP-106622, to Y.A.-G.; MOP-136834, to L.P.M.), the Natural Sciences and Engineering Research Council of Canada (J.G. and K.C.C.), the Canada Foundation for Innovation (K.C.C.), and the Michael Smith Foundation for Health Research (J.G.).

1. A. A. Hyman, C. A. Weber, F. Jülicher, Liquid-liquid phase separation in biology. *Annu. Rev. Cell Dev. Biol.* **30**, 39–58 (2014).
2. S. F. Banani, H. O. Lee, A. A. Hyman, M. K. Rosen, Biomolecular condensates: Organizers of cellular biochemistry. *Nat. Rev. Mol. Cell Biol.* **18**, 285–298 (2017).
3. Y. Shin, C. P. Brangwynne, Liquid phase condensation in cell physiology and disease. *Science* **357**, eaaf4382 (2017).
4. C. P. Brangwynne, P. Tompa, R. V. Pappu, Polymer physics of intracellular phase transitions. *Nat. Phys.* **11**, 899–904 (2015).
5. P. A. Chong, J. D. Forman-Kay, Liquid-liquid phase separation in cellular signaling systems. *Curr. Opin. Struct. Biol.* **41**, 180–186 (2016).
6. L. P. Bergeron-Sandoval, N. Safaee, S. W. Michnick, Mechanisms and consequences of macromolecular phase separation. *Cell* **165**, 1067–1079 (2016).
7. N. Al-Husini, D. T. Tomares, O. Bitar, W. S. Childers, J. M. Schrader, Alphaproteobacterial RNA degradosomes assemble liquid-liquid phase-separated RNP bodies. *Mol. Cell* **71**, 1027–1039.e14 (2018).
8. X. Su *et al*., Phase separation of signaling molecules promotes T cell receptor signal transduction. *Science* **352**, 595–599 (2016).
9. S. Banjade, M. K. Rosen, Phase transitions of multivalent proteins can promote clustering of membrane receptors. *eLife* **3**, e04123 (2014).
10. M. F. Garcia-Parajo, A. Cambi, J. A. Torreno-Pina, N. Thompson, K. Jacobson, Nanoclustering as a dominant feature of plasma membrane organization. *J. Cell Sci.* **127**, 4995–5005 (2014).
11. J. Goyette, K. Gaus, Mechanisms of protein nanoscale clustering. *Curr. Opin. Cell Biol.* **44**, 86–92 (2017).
12. E. Merklinger *et al*., The packing density of a supramolecular membrane protein cluster is controlled by cytoplasmic interactions. *eLife* **6**, e20705 (2017).
13. F. Heinkel *et al*., Biophysical characterization of the tandem FHA domain regulatory module from the Mycobacterium tuberculosis ABC transporter Rv1747. *Structure* **26**, 972–986.e6 (2018).
14. L. N. Glass *et al*., Mycobacterium tuberculosis universal stress protein Rv2623 interacts with the putative ATP binding cassette (ABC) transporter Rv1747 to regulate mycobacterial growth. *PLoS Pathog.* **13**, e1006515 (2017).
15. V. L. Spivey *et al*., Forkhead-associated (FHA) domain containing ABC transporter Rv1747 is positively regulated by Ser/Thr phosphorylation in Mycobacterium tuberculosis. *J. Biol. Chem.* **286**, 26198–26209 (2011).
16. R. M. Vernon *et al*., Pi-Pi contacts are an overlooked protein feature relevant to phase separation. *eLife* **7**, e31486 (2018).
17. S. Jain *et al*., ATPase-modulated stress granules contain a diverse proteome and substructure. *Cell* **164**, 487–498 (2016).
18. M. Feric *et al*., Coexisting liquid phases underlie nucleolar subcompartments. *Cell* **165**, 1686–1697 (2016).
19. J. Chao *et al*., Protein kinase and phosphatase signaling in Mycobacterium tuberculosis physiology and pathogenesis. *Biochim. Biophys. Acta* **1804**, 620–627 (2010).
20. S. Prisic *et al*., Extensive phosphorylation with overlapping specificity by Mycobacterium tuberculosis serine/threonine protein kinases. *Proc. Natl. Acad. Sci. U.S.A.* **107**, 7521–7526 (2010).
21. T. J. Nott *et al*., Phase transition of a disordered nuage protein generates environmentally responsive membraneless organelles. *Mol. Cell* **57**, 936–947 (2015).
22. J. M. Curry *et al*., An ABC transporter containing a forkhead-associated domain interacts with a serine-threonine protein kinase and is required for growth of Mycobacterium tuberculosis in mice. *Infect. Immun.* **73**, 4471–4477 (2005).
23. R. Durán *et al*., Conserved autophosphorylation pattern in activation loops and juxtamembrane regions of Mycobacterium tuberculosis Ser/Thr protein kinases. *Biochem. Biophys. Res. Commun.* **333**, 858–867 (2005).
24. J. Xu, Y. Liu, Y. Yang, S. Bates, J. T. Zhang, Characterization of oligomeric human half-ABC transporter ATP-binding cassette G2. *J. Biol. Chem.* **279**, 19781–19789 (2004).
25. F. Geillon *et al*., Peroxisomal ATP-binding cassette transporters form mainly tetramers. *J. Biol. Chem.* **292**, 6965–6977 (2017).
26. A. Abu-Arish *et al*., Cholesterol modulates CFTR confinement in the plasma membrane of primary epithelial cells. *Biophys. J.* **109**, 85–94 (2015).
27. D. Greenfield *et al*., Self-organization of the Escherichia coli chemotaxis network imaged with super-resolution light microscopy. *PLoS Biol.* **7**, e1000137 (2009).
28. G. B. Martins, G. Giacomelli, M. Bramkamp, Substrate-dependent cluster density dynamics in bacterial phosphotransferase system permeases. bioRxiv:10.1101/349514 (18 June 2018).
29. L. Pan *et al*., Higher-order clustering of the transmembrane anchor of DR5 drives signaling. *Cell* **176**, 1477–1489.e14 (2019).
30. R. Tafteh *et al*., Real-time 3D stabilization of a super-resolution microscope using an electrically tunable lens. *Opt. Express* **24**, 22959–22970 (2016).
31. R. Tafteh, D. R. Scriven, E. D. Moore, K. C. Chou, Single molecule localization deep within thick cells; a novel super-resolution microscope. *J. Biophotonics* **9**, 155–160 (2016).
32. M. Ester, H.-P. Kriegel, J. Sander, X. Xu, "A density-based algorithm for discovering clusters in large spatial databases with noise" in *Proceedings of the Second International Conference on Knowledge Discovery and Data Mining (KDD-96)*, E. Simoudis, J. Han, U. M. Fayyad, Eds., (AAAI Press, Menlo Park, CA, 1996), pp. 226–231.
33. M. B. Smolka *et al*., An FHA domain-mediated protein interaction network of Rad53 reveals its role in polarized cell growth. *J. Cell Biol.* **175**, 743–753 (2006).